

Angular distribution of hypersatellite and satellite radiation emitted after resonant transfer and excitation into U^{91+} ions

S. Zakowicz, Z. Harman,* N. Grün, and W. Scheid†

Institut für Theoretische Physik der Justus-Liebig-Universität Giessen, Heinrich-Buff-Ring 16, D-35392 Giessen, Germany

(Received 22 May 2003; published 23 October 2003)

In collisions of heavy few-electron projectile ions with light targets, an electron can be transferred from the target with the simultaneous excitation of a projectile electron. We study the angular distribution of deexcitation x rays following the resonant capture process. Our results are compared to experimental values of Ma *et al.* [Phys. Rev. A **68**, 042712 (2003)] for collisions of U^{91+} ions with a hydrogen gas target.

DOI: 10.1103/PhysRevA.68.042711

PACS number(s): 34.70.+e, 32.80.Hd, 31.30.Jv, 34.80.Lx

I. INTRODUCTION

Electron dynamics and interactions are strongly influenced in very heavy atomic systems by relativistic effects. The experimental investigation of resonant transfer and excitation (RTE) in highly charged ions is a suitable tool to study these phenomena [1,2]. In this process, a quasifree electron from a low- Z target atom is captured into an ion with the simultaneous excitation of a projectile electron, followed by the emission of stabilizing characteristic x-ray photons. The RTE process is closely related to dielectronic recombination (DR), in which an initially free electron is captured.

Relativistic effects are most pronounced for KLL transitions, where innershell electrons are involved. For hydrogenlike ions, the whole process including deexcitation by photon emission may be written as

$$1s_{1/2} + e^- \rightarrow [2l_j 2l'_{j'}]_{d_1} \rightarrow [1s_{1/2} 2l''_{j''}]_{d_2} + K\alpha^{\text{HS}} \rightarrow 1s^2 + K\alpha^{\text{HS}} + K\alpha^{\text{S}}. \quad (1)$$

Here, the first intermediate state d_1 decays into d_2 by emission of a hypersatellite (HS) photon, and then the ground state of the heliumlike system is reached by a satellite (S) transition. (For simplicity we omitted most reaction pathways with emission of more than two photons.) Alternatively, the second intermediate state d_2 can also be reached by radiative electron capture (REC), that is, capture with emission of a photon. X rays emitted following REC into the L -subshell levels give a sizeable contribution to the measured satellite intensities.

A similar RTE process was studied both experimentally [2] and theoretically [3] in the case of initially heliumlike uranium ions, where only one $K\alpha$ photon is emitted. The emission has been shown to be anisotropic due to the non-uniform occupation of the magnetic sublevels (the so-called alignment) of the states formed by resonant capture. It was also shown in Ref. [3] that the Breit term of the electron-electron interaction gives an observable important contribution to the parameters characterizing the anisotropy of dipole

emission. Balashov *et al.* [4] calculated general expressions for the angular anisotropy and correlation of cascade photons emitted in the DR and RTE processes. These authors supply numerical results only for a low- Z system, and their computations have not been experimentally verified yet.

In this paper we present calculations for the angular distributions of HS and S photons emitted during collisions of U^{91+} ions with a hydrogen gas target. The resulting intensity ratios are compared to those measured by Ma *et al.* [1]. Due to the narrow Compton profile of this target, the resonances in the cross sections have relatively small widths and can be resolved experimentally. In particular, the angular distribution of the radiation is only slightly blurred by overlapping resonances. Atomic units will be used throughout.

II. THEORY

A. Two-photon emission in the DR process

In Ref. [5], the triple-differential cross section for DR with two photon emissions is found to be

$$\begin{aligned} & \frac{d^3 \sigma_{\text{DR}}}{d\omega_1 d\Omega_1 d\Omega_2}(\omega_1; \theta_1, \phi_1, \theta_2, \phi_2) \\ &= \sum_{\substack{j,k=1 \\ j \neq k}}^2 \sum_{d_1, d_2} \frac{d\sigma_{\text{DR}}^{j,k}}{d\omega_1}(\omega_1; d_1, d_2) W_{d_1, d_2}^{j,k}(\theta_1, \phi_1, \theta_2, \phi_2). \end{aligned} \quad (2)$$

The angles $(\theta_1, \phi_1) \equiv \Omega_1$ and $(\theta_2, \phi_2) \equiv \Omega_2$ give the directions into which the photons are emitted. The z axis is chosen in the direction of the electron beam. Expression (2) is to be understood in such a way that the total DR cross section is

$$\sigma_{\text{DR}} = \frac{1}{2} \int d\omega_1 d\Omega_1 d\Omega_2 \frac{d^3 \sigma_{\text{DR}}}{d\omega_1 d\Omega_1 d\Omega_2}(\omega_1; \theta_1, \phi_1, \theta_2, \phi_2). \quad (3)$$

The summations in Eq. (2) are extended over the possible doubly excited (d_1) and singly excited (d_2) states as well as over the two possible time orders of photon emission. Note that cross section (2) is differential with respect to only *one* of the photon energies, which is labeled here as ω_1 . The energy ω_2 of the other photon is fixed by conservation of energy:

*Electronic address: zoltan.harman@theo.physik.uni-giessen.de

†URL: <http://service.physik.uni-giessen.de>

$$\omega_2 = E - E_f - \omega_1, \quad (4)$$

where E is the initial energy of the total system and E_f denotes the energy of the final atomic state without photons. We stress also that, since the two photons are indistinguishable particles, cross section (2) is symmetric with respect to an exchange of both the energies and angles of the photons:

$$\begin{aligned} & \frac{d^3 \sigma_{\text{DR}}}{d\omega_1 d\Omega_1 d\Omega_2}(\omega_1; \theta_1, \phi_1, \theta_2, \phi_2) \\ &= \frac{d^3 \sigma_{\text{DR}}}{d\omega_1 d\Omega_1 d\Omega_2}(E - E_f - \omega_1; \theta_2, \phi_2, \theta_1, \phi_1). \end{aligned} \quad (5)$$

Indeed, the variable ω_1 denotes only the energy of *one* of the two photons, which is not necessarily the one that is emitted first.

The partial cross sections in Eq. (2) have the form

$$\begin{aligned} & \frac{d\sigma_{\text{DR}}^{j,k}}{d\omega_1}(\omega_1; d_1, d_2) \\ &= \frac{2\pi^2}{p^2} \frac{A_r(d_2, f)}{\Gamma_{d_2}} \frac{A_r(d_1, d_2)}{\Gamma_{d_1}} V_a(d_1) \\ & \quad \times \frac{\Gamma_{d_1}/(2\pi)}{(E - E_{d_1})^2 + \Gamma_{d_1}^2/4} \frac{\Gamma_{d_2}/(2\pi)}{(E - E_{d_2} - \omega_j)^2 + \Gamma_{d_2}^2/4}, \end{aligned} \quad (6)$$

where ω_2 is determined according to Eq. (4). Here, p is the momentum of the incoming electron, E_{d_1} and E_{d_2} are the energies of the discrete intermediate states, and Γ_{d_1} and Γ_{d_2} their total widths. The quantities A_r are radiative transition rates between the bound atomic states, and $V_a(d_1)$ is the capture rate from the initial states i into the state d_1 given by

$$\begin{aligned} V_a(d_1) &= \frac{2\pi}{2(2J_i + 1)} \sum_{M_i m_s} \sum_{M_{d_1}} \int d\Omega_p |\langle d_1 J_{d_1} M_{d_1} | \\ & \quad \times V^C + V^B | i J_i M_i, \mathbf{p} m_s \rangle|^2 \rho_i, \end{aligned} \quad (7)$$

where J_i and J_{d_1} are the total angular momenta of the corresponding states and ρ_i is the state density at the initial state. The interaction of electrons 1 and 2 by exchanging a virtual photon of frequency ω is described by the sum of the Coulomb and generalized Breit operators:

$$V_{12}^C = \frac{1}{|\mathbf{r}_1 - \mathbf{r}_2|} \equiv \frac{1}{r_{12}}, \quad (8)$$

$$V_{12}^B = -\boldsymbol{\alpha}_1 \boldsymbol{\alpha}_2 \frac{\cos(\omega r_{12})}{r_{12}} + (\boldsymbol{\alpha}_1 \nabla_1)(\boldsymbol{\alpha}_2 \nabla_2) \frac{\cos(\omega r_{12}) - 1}{\omega^2 r_{12}}. \quad (9)$$

The latter accounts for retardation effects and magnetic interaction of the two Dirac currents. As Eq. (6) shows, the

order of magnitude of the energy-differential cross section is determined by branching ratios and capture rates, whereas the shape is given by the product of two Lorentz profiles. Expression (6) has been obtained by employing a projection operator formalism, which is given in Ref. [5] and will be presented in a future publication.

The functions $W_{d_1, d_2}^{j,k}$ in Eq. (2) give the angular dependence of the radiation of the cascades. They can be expanded in tensor products of spherical harmonics:

$$\begin{aligned} & W_{d_1, d_2}^{j,k}(\theta_1, \phi_1, \theta_2, \phi_2) \\ &= \frac{1}{4\pi} \sum_{\nu} \sum_{\nu_1, \nu_2} \beta_{(\nu_1, \nu_2)\nu}^{d_1, d_2, j, k} \{ \mathbf{Y}_{\nu_1}(\theta_1, \phi_1) \\ & \quad \otimes \mathbf{Y}_{\nu_2}(\theta_2, \phi_2) \}_{\nu, 0}. \end{aligned} \quad (10)$$

The coefficients β depend on the capture and radiative matrix elements, the partial-wave phases of the incoming electron, and the involved angular momenta. The explicit analytical form and further details on the calculation can be found in Ref. [5].

An integration of Eq. (2) over the angles of the photon with index 2 leads to the one-photon distribution

$$\frac{d^2 \sigma_{\text{DR}}}{d\omega d\Omega}(\omega; \theta, \phi) = \int d\Omega' \frac{d^3 \sigma_{\text{DR}}}{d\omega d\Omega d\Omega'}(\omega; \theta, \phi, \theta', \phi'), \quad (11)$$

which is of interest when only one of the photons is detected. A further calculation shows that

$$\frac{d^2 \sigma_{\text{DR}}}{d\omega d\Omega}(\omega; \theta, \phi) = \sum_{\substack{j,k=1 \\ j \neq k}}^2 \sum_{d_1, d_2} \frac{d\sigma_{\text{DR}}^{j,k}}{d\omega}(\omega; d_1, d_2) W_{d_1, d_2}^{j,k}(\theta, \phi), \quad (12)$$

where

$$\begin{aligned} & W_{d_1, d_2}^{1,2}(\theta, \phi) \equiv W_{d_1, d_2}^{1,2}(\theta) \\ &= \frac{1}{4\pi} \sum_{\nu} \sqrt{2\nu + 1} \beta_{(\nu, 0)\nu}^{d_1, d_2, 1, 2} P_{\nu}(\cos \theta) \end{aligned} \quad (13)$$

and

$$\begin{aligned} & W_{d_1, d_2}^{2,1}(\theta, \phi) \equiv W_{d_1, d_2}^{2,1}(\theta) \\ &= \frac{1}{4\pi} \sum_{\nu} \sqrt{2\nu + 1} \beta_{(\nu, 0)\nu}^{d_1, d_2, 2, 1} P_{\nu}(\cos \theta) \\ &= \frac{1}{4\pi} \sum_{\nu} \sqrt{2\nu + 1} \beta_{(\nu, 0)\nu}^{d_1, d_2, 1, 2} P_{\nu}(\cos \theta). \end{aligned} \quad (14)$$

In the last step in Eq. (14), the symmetry relation

$$\beta_{(\nu_1, \nu_2)\nu}^{d_1, d_2, 1, 2} = \beta_{(\nu_2, \nu_1)\nu}^{d_1, d_2, 2, 1} \quad (15)$$

has been used. P_ν are the Legendre polynomials of degree ν . We remark that Eq. (12) is still invariant under the transformation $\omega \mapsto E - E_f - \omega$, and that the total cross section is obtained from Eq. (2) by performing the following integration:

$$\sigma_{\text{DR}} = \frac{1}{2} \int_0^{E-E_f} d\omega \int d\Omega \frac{d^2 \sigma_{\text{DR}}}{d\omega d\Omega}(\omega; \theta, \phi). \quad (16)$$

B. Application to the RTE process

The electrons bound in the target molecule may be regarded as quasifree, and the impulse approximation is adopted [3,6]. Within this approximation, the effect of binding of electrons in the light target just gives rise to a momentum spread of the captured electron. In order to obtain the cross section for RTE, the DR cross section is convoluted with the electron momentum distribution in the target as seen from the projectile frame:

$$\frac{d^3 \sigma_{\text{RTE}}}{d\omega_1 d\Omega_1 d\Omega_2} = \frac{1}{4\pi} \int_0^\infty dq' I_0(q') \int d\Omega'_q \frac{d^3 \sigma_{\text{DR}}(\mathbf{q}(\mathbf{q}'))}{d\omega_1 d\Omega_1 d\Omega_2}. \quad (17)$$

The integration is performed over the electron momentum \mathbf{q}' in the target frame, whereas \mathbf{q} denotes the coordinates in the projectile frame. The distribution function $I_0(q')$ is an average over the direction of the molecule's symmetry axis and is thus spherically symmetric [7]. It is normalized to unity

$$\int d^3 q' \frac{I_0(q')}{4\pi q'^2} = \int_0^\infty dq' I_0(q') = 1. \quad (18)$$

Since we are only interested in the one-photon distribution here, we need the expression

$$\frac{d^2 \sigma_{\text{RTE}}}{d\omega d\Omega} = \frac{1}{4\pi} \int_0^\infty dq' I_0(q') \int d\Omega' \frac{d^2 \sigma_{\text{DR}}(\mathbf{q}(\mathbf{q}'))}{d\omega d\Omega} \quad (19)$$

instead of Eq. (17). Note that ω stands for the photon energy in the projectile frame. The angular-differential cross section for electron capture with emission of a certain spectral line—for example the $K\alpha_1^S$ line—is computed by integrating Eq. (19) over the energy of the photon and summing over the set of pairs (d_1, d_2) of states, which contribute to this line. We denote this set by \mathcal{D} . The main contributing states are listed in Table I.

In the specific case of *KLL*-RTE from a hydrogen gas target into hydrogenlike uranium ions, the width of the Compton profile is relatively large compared to the widths Γ and A_r of the atomic states appearing in Eq. (6). We therefore use δ functions instead of Lorentz profiles in this expression and approximate the angular-differential cross section for RTE by

$$\left(\frac{d\sigma_{\text{RTE}}}{d\Omega} \right)_{\mathcal{D}}(\theta) = \frac{1}{\gamma\nu} \sum_{\substack{j,k=1 \\ j \neq k}}^2 \sum_{(d_1, d_2) \in \mathcal{D}} W_{d_1, d_2}^{j,k}(\theta) R_{d_1, d_2}^{j,k} \mathcal{J}(q_z^{d_1}). \quad (20)$$

The quantities $R_{d_1, d_2}^{j,k}$ describe the strengths of the resonances [see Eq. (26)]. The Compton profile $\mathcal{J}(q_z)$ gives the probability density to find a target electron with the momentum component q_z in the projectile frame. It may be calculated from $I_0(q')$ by [7]

$$\mathcal{J}(q_z) = \int dq_x dq_y \frac{I_0(q'(\mathbf{q}))}{4\pi q'(\mathbf{q})^2} = \frac{1}{2} \int_{|q'_z(q_z)|}^\infty dq' \frac{I_0(q')}{q'}. \quad (21)$$

We obtained the Compton profile for the H_2 target by interpolating values tabulated by Jeziorski and Szalewicz *et al.* [8]. The momentum $q_z^{d_1}$ is found from the resonance energy E_{d_1} by a Lorentz transformation [3,6]:

$$q_z^{d_1} = \frac{\gamma(c^2 - |E_{\text{bind}}|) - (E_{d_1} - E_i + c^2)}{\gamma\nu}, \quad (22)$$

where E_{bind} is the binding energy of the electron in the target and E_i is the ground-state energy of the initial hydrogenlike ion.

If the natural line widths for the different lines are smaller than their energy separation, it is possible to distinguish between the two photons. This means that the photon with index 1 can indeed be regarded as the *first* photon (the hypersatellite). The angular-differential cross section is then found to be

$$\left(\frac{d\sigma_{\text{RTE}}}{d\Omega} \right)_{\mathcal{D}, i}(\theta) = \frac{1}{4\pi} \sigma_{\mathcal{D}, i}^{\text{RTE}} \sum_\nu \beta_{\mathcal{D}, i}^{\text{eff}, \nu} P_\nu(\cos \theta), \quad (23)$$

where i denotes the number of the photon which is detected. The partial cross sections appearing in Eq. (23) are given by

$$\sigma_{\mathcal{D}, 1}^{\text{RTE}} = \frac{1}{\gamma\nu} \sum_{(d_1, d_2) \in \mathcal{D}} R_{d_1, d_2} \mathcal{J}(q_z^{d_1}) \quad (24)$$

for the first photon and

$$\sigma_{\mathcal{D}, 2}^{\text{RTE}} = \frac{1}{\gamma\nu} \sum_{(d_1, d_2) \in \mathcal{D}} \frac{A_r(d_2, f)}{\Gamma_{d_2}} R_{d_1, d_2} \mathcal{J}(q_z^{d_1}) \quad (25)$$

for the second photon. The resonance strengths are

$$R_{d_1, d_2} := R_{d_1, d_2}^{1,2} = \frac{2\pi^2}{p^2} \frac{A_r(d_1, d_2)}{\Gamma_{d_1}} V_a(d_1), \quad (26)$$

and the effective anisotropy parameters in Eq. (23) are calculated by

$$\beta_{\mathcal{D}, 1}^{\text{eff}, \nu} = \sqrt{2\nu + 1} \left(\sum_{(d_1, d_2) \in \mathcal{D}} R_{d_1, d_2} \mathcal{J}(q_z^{d_1}) \right)^{-1} \times \sum_{(d_1, d_2) \in \mathcal{D}} R_{d_1, d_2} \mathcal{J}(q_z^{d_1}) \beta_{(\nu, 0)\nu}^{d_1, d_2, 1, 2} \quad (27)$$

TABLE I. Intermediate states d_1 and d_2 , their energies E_{d_1} and E_{d_2} , labeling of the photons, and resonance strengths R_{d_1, d_2} for the most dominant cascades. (The dashes indicate that the emitted radiation belongs neither to the $K\alpha_1^{\text{HS}}$ nor to the $K\alpha_2^{\text{HS}}$ energy range.)

Resonance group	State d_1	E_{d_1} (eV)	First photon	State d_2	E_{d_2} (eV)	Second photon	R_{d_1, d_2} (b eV)	$\Sigma_{d_2} R_{d_1, d_2}$ (b eV)
$KL_{1/2}L_{1/2}$	$[2s_{1/2}2p_{1/2}]_0$	-67896	$K\alpha_2^{\text{HS}}$	$[1s_{1/2}2s_{1/2}]_1$	-165369	$K\alpha_2^{\text{S}}$	18142	18215
			$K\alpha_2^{\text{HS}}$	$[1s_{1/2}2p_{1/2}]_1$	-165225	$K\alpha_2^{\text{S}}$	72.9	
	$[2s_{1/2}2s_{1/2}]_0$	-67833	$K\alpha_2^{\text{HS}}$	$[1s_{1/2}2s_{1/2}]_1$	-165369	$K\alpha_2^{\text{S}}$	54.9	15924
			$K\alpha_2^{\text{HS}}$	$[1s_{1/2}2p_{1/2}]_1$	-165225	$K\alpha_2^{\text{S}}$	15868	
			—	$[1s_{1/2}2p_{3/2}]_1$	-160783	$K\alpha_1^{\text{S}}$	1.03	
	$[2s_{1/2}2p_{1/2}]_1$	-67856	$K\alpha_2^{\text{HS}}$	$[1s_{1/2}2s_{1/2}]_1$	-165369	$K\alpha_2^{\text{S}}$	14158	20841
			$K\alpha_2^{\text{HS}}$	$[1s_{1/2}2p_{1/2}]_1$	-165225	$K\alpha_2^{\text{S}}$	55.9	
			$K\alpha_2^{\text{HS}}$	$[1s_{1/2}2p_{1/2}]_0$	-165114	$K\alpha_2^{\text{S}}$	27.9	
			$K\alpha_2^{\text{HS}}$	$[1s_{1/2}2s_{1/2}]_0$	-165113	$K\alpha_2^{\text{S}}$	6599	
	$[2p_{1/2}2p_{1/2}]_0$	-67712	$K\alpha_2^{\text{HS}}$	$[1s_{1/2}2s_{1/2}]_1$	-165369	$K\alpha_2^{\text{S}}$	32.8	6937
			$K\alpha_2^{\text{HS}}$	$[1s_{1/2}2p_{1/2}]_1$	-165225	$K\alpha_2^{\text{S}}$	6902	
			—	$[1s_{1/2}2p_{3/2}]_1$	-160783	$K\alpha_1^{\text{S}}$	2.20	
$KL_{1/2}L_{3/2}$	$[2s_{1/2}2p_{3/2}]_2$	-63393	$K\alpha_1^{\text{HS}}$	$[1s_{1/2}2s_{1/2}]_1$	-165369	$K\alpha_2^{\text{S}}$	5462	5504
			$K\alpha_1^{\text{HS}}$	$[1s_{1/2}2s_{1/2}]_0$	-165113	$K\alpha_2^{\text{S}}$	15.1	
			$K\alpha_2^{\text{HS}}$	$[1s_{1/2}2p_{3/2}]_2$	-160857	$K\alpha_1^{\text{S}}$	13.3	
			$K\alpha_2^{\text{HS}}$	$[1s_{1/2}2p_{3/2}]_1$	-160783	$K\alpha_1^{\text{S}}$	13.3	
	$[2p_{1/2}2p_{3/2}]_1$	-63355	$K\alpha_1^{\text{HS}}$	$[1s_{1/2}2p_{1/2}]_1$	-165225	$K\alpha_2^{\text{S}}$	334	2164
			$K\alpha_1^{\text{HS}}$	$[1s_{1/2}2p_{1/2}]_0$	-165114	$K\alpha_2^{\text{S}}$	651	
			$K\alpha_2^{\text{HS}}$	$[1s_{1/2}2p_{3/2}]_2$	-160857	$K\alpha_1^{\text{S}}$	984	
			$K\alpha_2^{\text{HS}}$	$[1s_{1/2}2p_{3/2}]_1$	-160783	$K\alpha_1^{\text{S}}$	195	
	$[2p_{1/2}2p_{3/2}]_2$	-63339	$K\alpha_1^{\text{HS}}$	$[1s_{1/2}2p_{1/2}]_1$	-165225	$K\alpha_2^{\text{S}}$	8579	19004
			$K\alpha_1^{\text{HS}}$	$[1s_{1/2}2p_{1/2}]_0$	-165114	$K\alpha_2^{\text{S}}$	24.0	
			$K\alpha_2^{\text{HS}}$	$[1s_{1/2}2p_{3/2}]_2$	-160857	$K\alpha_1^{\text{S}}$	5266	
			$K\alpha_2^{\text{HS}}$	$[1s_{1/2}2p_{3/2}]_1$	-160783	$K\alpha_1^{\text{S}}$	5135	
$[2s_{1/2}2p_{3/2}]_1$	-63268	$K\alpha_1^{\text{HS}}$	$[1s_{1/2}2s_{1/2}]_1$	-165369	$K\alpha_2^{\text{S}}$	2671	8384	
		$K\alpha_1^{\text{HS}}$	$[1s_{1/2}2s_{1/2}]_0$	-165113	$K\alpha_2^{\text{S}}$	5672		
		$K\alpha_2^{\text{HS}}$	$[1s_{1/2}2p_{3/2}]_2$	-160857	$K\alpha_1^{\text{S}}$	33.8		
		$K\alpha_2^{\text{HS}}$	$[1s_{1/2}2p_{3/2}]_1$	-160783	$K\alpha_1^{\text{S}}$	6.75		
$KL_{3/2}L_{3/2}$	$[2p_{3/2}2p_{3/2}]_2$	-58828	$K\alpha_1^{\text{HS}}$	$[1s_{1/2}2p_{3/2}]_2$	-160857	$K\alpha_1^{\text{S}}$	3650	7351
			$K\alpha_1^{\text{HS}}$	$[1s_{1/2}2p_{3/2}]_1$	-160783	$K\alpha_1^{\text{S}}$	3701	
	$[2p_{3/2}2p_{3/2}]_0$	-58733	$K\alpha_1^{\text{HS}}$	$[1s_{1/2}2p_{3/2}]_2$	-160857	$K\alpha_1^{\text{S}}$	9.10	1302
			$K\alpha_1^{\text{HS}}$	$[1s_{1/2}2p_{3/2}]_1$	-160783	$K\alpha_1^{\text{S}}$	1293	

$$\beta_{D,2}^{\text{eff},\nu} = \sqrt{2\nu+1} \left(\sum_{(d_1, d_2) \in \mathcal{D}} \frac{A_r(d_2, f)}{\Gamma_{d_2}} R_{d_1, d_2} \mathcal{J}(q_z^{d_1}) \right)^{-1} \times \sum_{(d_1, d_2) \in \mathcal{D}} \frac{A_r(d_2, f)}{\Gamma_{d_2}} R_{d_1, d_2} \mathcal{J}(q_z^{d_1}) \beta_{(0,\nu)v}^{d_1, d_2, 1, 2}. \quad (28)$$

III. NUMERICAL RESULTS AND DISCUSSION

The relativistic resonance energies, bound-state wave functions, and the radiative transition rates are obtained with the GRASP multiconfigurational Dirac-Fock atomic structure code by Dyall *et al.* [9]. Nuclear finite-size effects are taken

into account by using a two-parameter Fermi charge distribution. Lowest-order QED corrections are included in the energies in an approximate manner.

A partial-wave expansion is used for the wave function of the incoming electron with asymptotic momentum \mathbf{p} and spin projection m_s :

$$\psi_{\mathbf{p}m_s}(\mathbf{r}) = \sum_{\kappa\mu} i^l e^{i\Delta_\kappa} \sum_{m_l} Y_l^{m_l*}(\hat{\mathbf{p}}) C\left(l \frac{1}{2} j; m_l m_s \mu\right) \psi_{p\kappa\mu}(\mathbf{r}). \quad (29)$$

The partial-wave components $\psi_{p\kappa\mu}(\mathbf{r})$ are calculated numerically by integrating the Dirac equation with the nuclear potential screened by the bound $1s$ electron. This task and

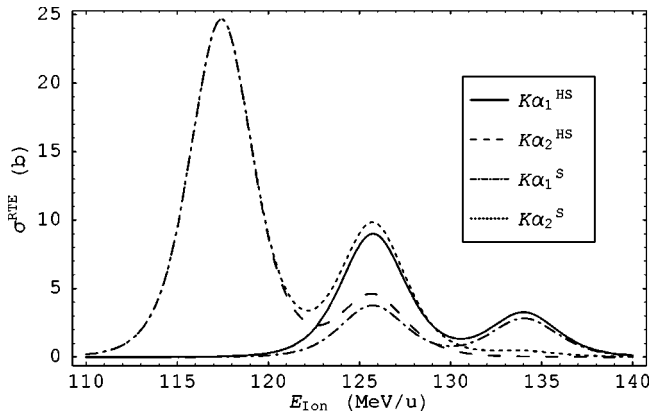


FIG. 1. Partial RTE cross sections for emission of $K\alpha_1$ and $K\alpha_2$ radiation in the range of the KLL resonances as function of uranium lab energy.

the evaluation of matrix elements for the capture of the continuum electron are performed by the Auger code of Zimmerer [10].

The phases Δ_κ in Eq. (29) ensure that the wave function satisfies the boundary condition of an incoming plane wave and an outgoing spherical wave. They are determined by matching the numerical solution integrated in the interior region with analytic Dirac-Coulomb functions of the exterior region.

The theory developed above will now be applied to a comparison with the experiment performed by Ma *et al.* [1], who observed the x-ray emission after collisions of U^{91+} ions with a hydrogen gas target. We consider here intensity ratios since they are experimentally accessible with a larger precision than absolute cross sections.

Partial RTE cross sections for $K\alpha_1$ ($2p_{3/2} \rightarrow 1s_{1/2}$) and $K\alpha_2$ ($2s_{1/2}, 2p_{1/2} \rightarrow 1s_{1/2}$) radiation as calculated with Eq. (24) are shown in Fig. 1. Within the resonance groups, the single DR resonances listed in Table I cannot be resolved since they are broadened by the target Compton profile. The values of the partial cross sections at the experimental energies are displayed in Table II and are compared to the measurement in Table II of the companion paper [1]. Note that the cross sections are understood with respect to one target electron.

Figure 2 shows the effective dipole anisotropy parameters $\beta_{D,i}^{\text{eff},\nu=2}$ introduced in Eqs. (27) and (28) selectively for $K\alpha_1$ and $K\alpha_2$ emission in the energy range of KLL transitions. Note that only dipole radiation was regarded in these calculations, in which case Eq. (23) becomes

TABLE II. Partial cross sections $\sigma_{D,1}^{\text{RTE}}$ for the first photon (hypersatellite, HS) and $\sigma_{D,2}^{\text{RTE}}$ for the second photon (satellite, S) in barn.

Projectile energy (MeV/u)	$K\alpha_1^{\text{HS}}$	$K\alpha_2^{\text{HS}}$	$K\alpha_1^{\text{S}}$	$K\alpha_2^{\text{S}}$
116.6	0.0299	21.7	0.0141	21.7
124.9	7.94	4.22	3.35	8.81
133.1	2.90	0.0644	2.48	0.481

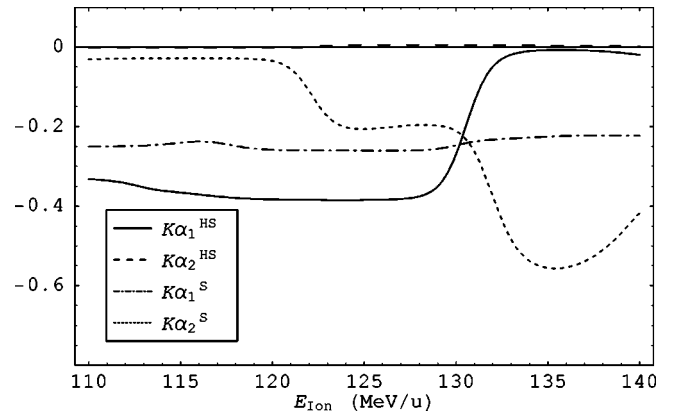


FIG. 2. Effective dipole anisotropy parameters $\beta_{D,i}^{\text{eff},2}$ for HS ($i=1$) and S ($i=2$) emission as function of the ion energy in the range of the KLL resonances.

$$\begin{aligned} \left(\frac{d\sigma_{D,i}^{\text{RTE}}}{d\Omega} \right) (\theta) &= \frac{1}{4\pi} \sigma_{D,i}^{\text{RTE}} [1 + \beta_{D,i}^{\text{eff},2} P_2(\cos \theta)] \\ &= \frac{1}{4\pi} \sigma_{D,i}^{\text{RTE}} \left[1 + \frac{1}{2} \beta_{D,i}^{\text{eff},2} (3\cos^2 \theta - 1) \right]. \end{aligned} \quad (30)$$

For the cascades via the singly excited $[1s_{1/2}2p_{3/2}]_2$ state, which decays first into the state $[1s_{1/2}2s_{1/2}]_1$ with a branching ratio of around 30%, the *third* photon is the satellite. The anisotropy of this photon is also incorporated in the numerical results. The values of the effective anisotropy parameters at the experimental energies are listed in Table III. At a projectile energy of 116.6 MeV, which is in the range of the $KL_{1/2}L_{1/2}$ resonance group, the $K\alpha_1^{\text{HS}}$ emission is strongly anisotropic.

In Fig. 3, the ratio of the $K\alpha_1$ and $K\alpha_2$ HS intensities is plotted against the emission angle in the laboratory frame at 124.9 MeV/u, which corresponds to $KL_{1/2}L_{3/2}$ resonances. Hypersatellite lines are not perturbed by the REC contribution since the doubly excited states from which they are emitted can only be populated by RTE. A comparison with Fig. 2 reveals that the $K\alpha_2^{\text{HS}}$ line is isotropic. This is confirmed by the measurements (see Fig. 8 and the related discussion in Ref. [1]). Therefore the anisotropy of the intensity ratio stems from the $K\alpha_1^{\text{HS}}$ radiation. The theoretical curve is in qualitative agreement with the experimental data from Ref. [1]. However, our calculation underestimates the intensity ratios at 60° and 90° . This deviation might be removed

TABLE III. Effective dipole anisotropy parameters $\beta_{D,1}^{\text{eff},2}$ for the first photon (hypersatellite, HS) and $\beta_{D,2}^{\text{eff},2}$ for the second photon (satellite, S).

Projectile energy (MeV/u)	$K\alpha_1^{\text{HS}}$	$K\alpha_2^{\text{HS}}$	$K\alpha_1^{\text{S}}$	$K\alpha_2^{\text{S}}$
116.6	-0.374	-2.02×10^{-3}	-0.239	-0.0286
124.9	-0.384	5.18×10^{-3}	-0.260	-0.206
133.1	-0.0177	4.58×10^{-3}	-0.230	-0.493

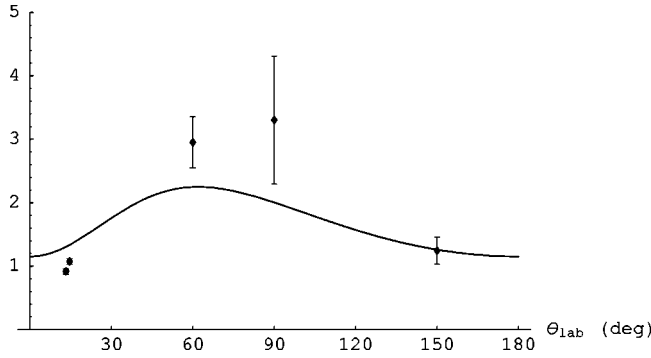


FIG. 3. Ratio of the $K\alpha_1^{\text{HS}}$ and $K\alpha_2^{\text{HS}}$ intensities at an ion energy of 124.9 MeV/u. Experimental values were taken from Ref. [1].

by taking into account interferences between different multipole orders of the radiation. Surzhykov *et al.* [11] showed how the interference between $E1$ and $M2$ transitions in the $K\alpha_1$ decay in hydrogenlike heavy ions may modify the angular distributions of the emitted photons when an alignment in the L -shell is present. The RTE process also produces aligned states.

Figures 4 and 5 show the angular distribution of the $K\alpha_1^{\text{HS}}$ and $K\alpha_2^{\text{HS}}$ radiation in the $KL_{1/2}L_{3/2}$ resonance group. The experimental data points have been normalized to the measured angular distribution of the $K\alpha_2^{\text{S}}$ radiation, which has been proven experimentally to be isotropic for all the resonance groups, even at a nonresonant projectile energy (see Fig. 6 and explanations in Ref. [1]). Although we have found that the $K\alpha_2^{\text{S}}$ emission of the RTE process possesses a strong angular dependence (see Fig. 2 and Table III), the total $K\alpha_2^{\text{S}}$ intensity is dominated by isotropically emitted photons following REC into the L -shell or higher shells. Therefore the $K\alpha_2^{\text{S}}$ radiation can be regarded as isotropic at the level of experimental accuracy. In our calculation we adjusted the angular-independent cross section $\sigma_{K\alpha_2^{\text{S}}}^{\text{REC}}$ of the deexcitation x rays from REC in order to fit the experimental intensity ratios. Neglecting interferences between RTE and REC, we have

$$\frac{(d\sigma/d\Omega)_{K\alpha_1^i}(\theta)}{(d\sigma/d\Omega)_{K\alpha_2^{\text{S}}}(\theta)} = \frac{\sigma_{K\alpha_1^i}^{\text{RTE}}[1 + \beta_{K\alpha_1^i}P_2(\cos\theta)]}{\sigma_{K\alpha_2^{\text{S}}}^{\text{RTE}}[1 + \beta_{K\alpha_2^{\text{S}}}P_2(\cos\theta)] + \sigma_{K\alpha_2^{\text{S}}}^{\text{REC}}}, \quad (31)$$

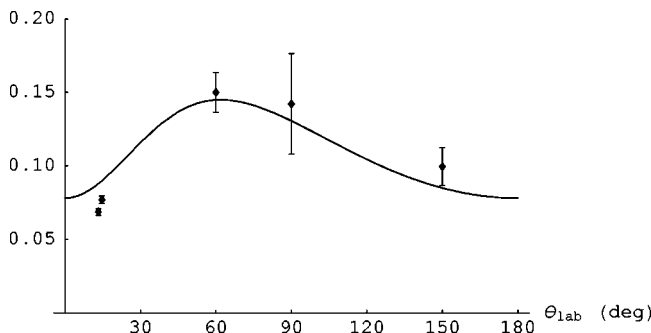


FIG. 4. Ratio of the $K\alpha_1^{\text{HS}}$ and $K\alpha_2^{\text{S}}$ intensities at an ion energy of 124.9 MeV/u. Experimental values were taken from Ref. [1].

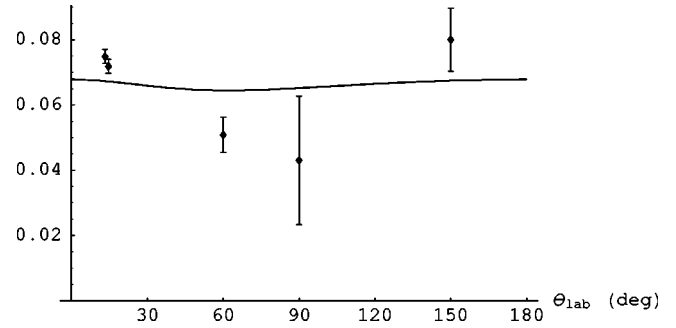


FIG. 5. Ratio of the $K\alpha_2^{\text{HS}}$ and $K\alpha_2^{\text{S}}$ intensities at an ion energy of 124.9 MeV/u. Experimental values were taken from Ref. [1].

where i stands for HS or S, and the value $\sigma_{K\alpha_2^{\text{S}}}^{\text{REC}} = 55.6$ b is found. So this analysis also yields an estimate for the REC cross section, showing that it indeed overweighs the RTE cross section of 8.8 b. With the above value, we see a reasonable agreement between experiment and theory, in particular in Fig. 4.

Figure 6 contains the angular distribution of $K\alpha_1^{\text{HS}}$ radiation emitted in the range of the $KL_{3/2}L_{3/2}$ group. Here we followed the same normalization procedure as explained for the previous figures and found the REC cross section $\sigma_{K\alpha_2^{\text{S}}}^{\text{REC}} = 74.6$ b. Comparing this to the RTE contribution of only 0.5 b, we can conclude that the REC process is even more dominant for the third resonance group. The agreement is again satisfactory within the experimental errors.

IV. SUMMARY

In this paper we studied the angular distribution of radiation emitted after KLL -RTE into U^{91+} ions. The dipole coefficients for the radiation appearing in the expansion in coupled spherical harmonics were calculated explicitly. From this expansion, both hypersatellite and satellite angular distributions were obtained. We applied the impulse approximation to compute differential cross sections for RTE in collisions of uranium ions with a hydrogen-molecule gas target. The comparison of our results to experimental data shows a good qualitative agreement. A future extension of this work should also account for interference effects with higher multipole orders of the radiation.

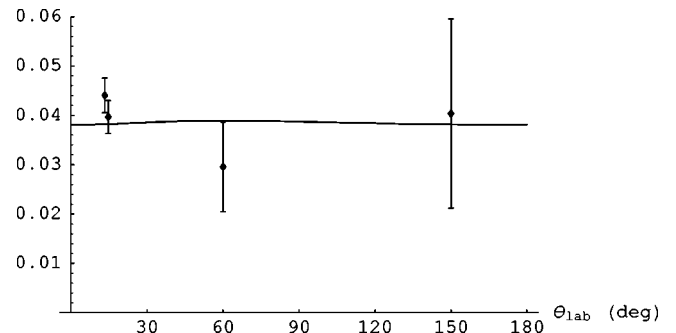


FIG. 6. Ratio of the $K\alpha_1^{\text{HS}}$ and $K\alpha_2^{\text{S}}$ intensities at an ion energy of 133.1 MeV/u. Experimental values were taken from Ref. [1].

The studies presented here give detailed information about the alignment of intermediate states after the KLL -RTE capture into U^{91+} and, therefore, lead to a deeper understanding of the electron-electron interaction in the dynamics of the capture process. In this context, we point out the importance of the Breit interaction for a capture in the $KL_{1/2}L_{1/2}$ resonance group. We note that our calculations also help us to analyze the experimental spectra by examining the angular distribution of the radiation.

In summary, these investigations provide a clear interpretation of the capture process and the following photon emissions.

ACKNOWLEDGMENTS

The authors would like to thank the experimental colleagues Professor P. Mokler at GSI Darmstadt and Professor X. Ma at IMP Lanzhou for stimulating discussions.

-
- [1] X. Ma *et al.*, Phys. Rev. A **68**, 042712 (2003).
[2] Th. Kandler *et al.*, Phys. Lett. A **204**, 274 (1995).
[3] M. Gail, N. Grün, and W. Scheid, J. Phys. B **31**, 4645 (1998).
[4] V.V. Balashov, I.V. Bodrenko, V.K. Dolinov, and S.I. Strakhova, Opt. Spectrosc. **77**, 801 (1994).
[5] S. Zakowicz, Diploma thesis, University of Giessen, 2001 (unpublished); S. Zakowicz, W. Scheid, and N. Grün, Nucl. Instrum. Methods Phys. Res. B **205**, 386 (2003).
[6] J. Eichler and W. E. Meyerhof, *Relativistic Atomic Collisions* (Academic Press, San Diego, 1995).
[7] R.E. Brown and V.H. Smith, Phys. Rev. A **5**, 140 (1972).
[8] B. Jeziorski and K. Szalewicz, Phys. Rev. A **19**, 2360 (1979).
[9] K.G. Dylla, I.P. Grant, C.T. Johnson, F.A. Parpia, and E.P. Plummer, Comput. Phys. Commun. **55**, 425 (1989).
[10] P. Zimmerer, N. Grün, and W. Scheid, Phys. Lett. A **148**, 457 (1990).
[11] A. Surzhykov, S. Fritzsche, A. Gumberidze, and Th. Stöhlker, Phys. Rev. Lett. **88**, 153001 (2002).